Temperature of artificial freshwater recharge significantly affects salinity distributions in coastal confined aquifers

Li Pu[1], Pei Xin[1, 2 #], Xiayang Yu[1], Ling Li[3], D. A. Barry[4]

[1]State Key Laboratory of Hydrology-Water Resources and Hydraulic Engineering, Hohai University, Nanjing, China

[2]Yangtze Institute for Conservation and Development, Hohai University, Nanjing, China

[3]School of Engineering, Westlake University, Hangzhou, China

[4]Laboratoire de technologie écologique (ECOL), Institut d'ingénierie de l'environnement (IIE), Faculté de l'environnement naturel, architectural et construit (ENAC), Ecole Polytechnique Fédérale de Lausanne (EPFL), Lausanne, Switzerland

[#]Corresponding author: Pei Xin, State Key Laboratory of Hydrology-Water Resources and Hydraulic Engineering, Hohai University, Nanjing, China. (xinpei@hhu.edu.cn)

Key points

- Hot/cold freshwater recharge induces a landward/seaward saltwater wedge
- Hot freshwater recharge induces a temporal overshoot of salinity distribution
- Response of salinity distribution to cold freshwater recharge is prolonged

Abstract

Artificial freshwater recharge is commonly used to mitigate seawater intrusion and restore salinized aquifers in coastal zones. While the temperature of recharged freshwater often differs from that of aquifers, effects of temperature differences on water flow and salinity distributions are rarely examined. Based on laboratory experiments and numerical simulations, we found that the response of salinity distribution to cold freshwater recharge is prolonged. Cold freshwater recharge performs better compared with hot water in mitigating seawater intrusion in confined aquifers. Hot freshwater recharge induces a marked overshoot of salinity distribution: Seawater retreats first but intrudes back until a steady state.

Keywords: aquifer; temperature; seawater intrusion; artificial freshwater recharge; coastal zone

1. Introduction

Coastal aquifers provide important freshwater resources in low-lying coastal areas (Barlow & Reichard, 2009; Costall et al., 2020). Generally, freshwater lays above the denser seawater in aquifers with saltwater wedges formed near the coastline (Figure 1a) (Werner et al., 2013). This equilibrium is vulnerable to reduced inland freshwater input, excessive groundwater extraction and sea level rise, which decrease seaward hydraulic gradients (Ferguson & Gleeson, 2012;

Robinson et al., 2018; Werner et al., 2013). As a result, denser seawater intrudes further landward and contaminates inland groundwater, threatening coastal communities and agriculture relying on fresh groundwater supplies (Ballesteros et al., 2016; Singh, 2014).

Various strategies (e.g., optimization of groundwater utilization, artificial freshwater recharge, construction of physical barriers) are used to mitigate seawater intrusion and restore salinized aquifers (Abd-Elhamid & Javadi, 2011; Hussain et al., 2019; Luyun et al., 2011). Among them, artificial freshwater recharge is practical and cost-effective, and has been widely adopted for several decades, e.g., in USA (Barlow & Reichard, 2009), Australia (Werner, 2009) and China (Shi & Jiao, 2014). For confined aquifers, freshwater is commonly injected into the subsurface through injection wells. The recharged freshwater increases the seaward hydraulic gradient and pushes the saltwater wedge seaward.

Water flow and salinity distributions in coastal aquifers have been extensively studied (Mao et al., 2006; Robinson et al., 2018; Werner et al., 2013), in particular, the performance of artificial freshwater recharge has been examined by analytical solutions (Hunt, 1985; Lu et al., 2017), laboratory experiments (Botero-Acosta & Donado, 2015; Luyun et al., 2011), numerical simulations (Armanuos et al., 2020; Mahesha, 1996a, 1996b) and field investigations (Bouri & Dhia, 2010). These studies show that artificial freshwater recharge is an efficient method of combating seawater intrusion in both unconfined and confined aquifers, the performance of which depends on well location, freshwater recharge rate and aquifer properties.

Previous studies on artificial freshwater recharge overlooked the temperature difference between recharged freshwater and aquifers. Analytical solutions and numerical simulations assume of isothermal conditions. In practice, recharged freshwater is often from the land surface (e.g., surface water in the wet season, treated wastewater or desalinated seawater). Its

temperature is expected to differ from that of deep aquifers, which is relatively stable. As fluid density and viscosity depend on temperature (Jamshidzadeh et al., 2013; Van Lopik et al., 2015), the recharged freshwater changes both thermal regime and physical properties of aquifers. The two are expected to alter the spatio-temporal water flow and salinity distributions in aquifers.

Recently, Pu et al. (2020) examined thermal effects on salinity distributions in confined aquifers. They found that as temperature of inland freshwater input increases, the freshwater-seawater interface intrudes landward and thus the freshwater storage decreases in confined aquifers. While this study demonstrated the importance of thermal state, it focused on steady conditions. The salinity distributions in response to artificial freshwater recharge with changing thermal regimes remain unknown. In this study, we conducted both laboratory experiments and numerical simulations on transient coupled flow, salt and heat transport in confined aquifers. The dynamic salinity distributions in response to the recharged freshwater with different temperatures were examined.

2. Methods

The laboratory experiments were conducted in an indoor heat-insulating flume (2.2-m long, 1.0-m high and 0.1-m thick) linked to two temperature-controlled water tanks that stored freshwater and seawater separately (Figure 1b, as used by Pu et al. (2020)). The flume had two side compartments used for setting up a fixed-flux boundary (landward) and a watertable-controlled boundary (seaward), respectively. In the flume, an essentially 2D confined aquifer was created with a 1.96-m long and 0.5-m deep quartz sand layer overlain by a 0.15-m deep clay layer (parameters are listed in Table 1). The overall setup is similar to the Henry problem (Henry, 1964), which is a benchmark for testing density-dependent groundwater flow in confined

aquifers. A thin tube (behaves as a recharge well) wrapped with insulating material was inserted into the aquifer with its outlet at x = -1.25 m and z = 0.25 m (note that the x-z coordinate origin is set at the impervious base and the seaside aquifer, Figure S1, S refers to supplementary materials). An array of digital thermometers (Dallas Semiconductors DS18B20) was installed in the seaside aquifer to detect the temperature distributions. One thermometer was also set up at the outlet of the recharge well to measure the temperature of the injected water (locations of thermometers in supplementary materials, Figure S1).

Prior to the freshwater recharge, the flow and salinity distribution at a steady state were established through the flume with a constant flux of 900 ml/min/m at the landward boundary (salinity was set to 0 ppt (mass fraction, parts per thousand)) and the seawater (salinity was set to 35 ppt) level fixed at 0.61 m (above the aquifer base). Both the freshwater and seawater temperatures were set to 25°C. To minimize heat dissipation, an air conditioner was used to maintain the ambient temperature at approximately 25°C. The seawater wedge movement was visualized by mixing seawater with FD&C red food dye. When the salinity distribution reached steady state, freshwater mixed with FD&C blue food dye was injected into the confined aquifer at a flux of 540 ml/min/m. Three independent experiments considering cold (temperature of recharged water, T_{in} = 10°C), isothermal (T_{in} = 25°C), and hot (T_{in} = 40°C) injection water were conducted.

During the experiments, digital color photographs were taken at an interval of 120 s to track the movement of injected water (blue color) and variation of saltwater wedge (red color). The photographs were processed by calculating the optimum hue threshold values using the rgb2hsv function in MATLAB to delineate the freshwater-seawater interfaces. This dye-tracking method has been widely used to track salinity distributions in sand flumes (Chang & Clement, 2012,

2013; Goswami & Clement, 2007; Kuan et al., 2012) and is particularly applicable for those with narrow mixing zones of saltwater and freshwater.

Direct measurements of the effects of temperature on in situ fluid and aquifer properties are infeasible, so for additional insights 2D numerical simulations of flow and coupled solute and heat transport using SUTRA-MS (Hughes & Sanford, 2004) were conducted. The governing equation is based on Darcy's law and considers saturated flow and soil and water compressibility. A unified solute- and heat-balance equation is used to solve both solute and heat transport. The boundary conditions were consistent with the experimental setup. Both laboratory-scale (parameters are listed in Table 1; the aquifer was assumed to be homogeneous and isotropic) and large-scale confined aquifers (both homogenous and heterogeneous) were simulated (details in supplementary materials).

3. Results and discussions

Initially (Hour 0, prior to the freshwater recharge), similar saltwater wedges formed for the three cases and the toe locations (intersection of the freshwater-seawater interface and the aquifer base) were all at x = -0.92 m (Figure 2). The continuously-injected freshwater formed seaward-directed (blue) plumes. Injecting water into the freshwater zone inhibits seawater intrusion since it increases both the total freshwater discharge to the "sea" and the lateral hydraulic gradient (Werner et al., 2013). The experimental results were consistent with this as for all three cases the freshwater-seawater interface retreated seaward and eventually reached a new steady state. For example, the toe location for hot-water injection (T_{in} = 40°C) retreated to -0.66 m after Hour 6 (Figure 2). For the three different T_{in} values, the steady-state plume shapes of the injected freshwater did not differ significantly (blue plumes in Figure 2). However, the cold injected

freshwater induced a smaller saltwater wedge. As T_{in} was changed from 40°C to 25°C and 10°C (warm, isothermal, cold), the toe location changed from -0.66 to -0.56 and -0.47 m (Figure 2, Hour 10). We also calculated the saltwater wedge areas (areas enclosed by the freshwater-seawater interfaces, aquifer base and seaward boundary), which decreased from 0.101 to 0.082 and 0.064 m^2 as T_{in} changed from 40°C to 25°C and 10°C, i.e., cold-water recharge performed the best in mitigating seawater intrusion. This difference was major as the distance from the toe location to the seaward boundary for T_{in} = 40°C (0.66 m) was 1.4 times larger than that for T_{in} = 10°C (0.47 m), while the saltwater wedge area almost doubled (0.101 vs. 0.064 m^2).

Overall, the numerical simulations (the freshwater-seawater interface was considered as the 50% seawater salinity isoline, 17.5 ppt) well reproduced the variations of toe locations observed in the experiments but overpredicted the area of the saltwater wedge after the freshwater recharge (after Hour 2, Figure 3). The difference may be due to heat dissipation (Figure S2) and the uncertainty involved in the experimental measurements (e.g., tracking salinity distributions using dyes). Nevertheless, the trends of the experimental and simulation results were consistent, which allowed us to explore the underlying mechanisms based on the numerical simulations. With the freshwater injection, the simulated toe location moved seaward and the area of the saltwater wedge decreased quickly (Hour 0 to Hour 2, Figure 3) on the same characteristic time scale as in the experiments. Afterwards, the two measures (toe location and area of saltwater wedge) reached steady state (defined operationally as no observable change). For the cases with T_{in} = 25°C and 10°C, the experimental data (Figure 3) for both toe location and area of saltwater wedge decreased approximately monotonically (decreasing rapidly at first and then approaching the steady state). For the cold-water case, the response time to reach the final steady state (operationally defined as the time to reach 95% toe location difference between the beginning

and final steady state conditions as done by Watson et al. (2010)) was around 6 h and lagged behind that for the isothermal case (around 3.5 h), suggesting that the thermal regime changed the flow and salt transport that allowed the aquifer to take more time to re-equilibrate. Since, with a temperature decrease, the fluid viscosity increases and thus the hydraulic conductivity decreases (Hughes & Sanford, 2004), e.g., as temperature increased from 10°C to 25°C and 40°C, the freshwater hydraulic conductivity increased from 0.0035 to 0.0051 and 0.0069 m/s for the considered aquifer. This would decrease the freshwater flow and slow down the response of the saltwater wedge to freshwater recharge. The effects of coupled salt and heat transport is evident for the hotter case (T_{in} = 40°C); both the toe location and area of saltwater wedge decreased first (toe location moved from -0.92 to -0.61 m from Hour 0 to 3.4) but bounced back (toe location moved from -0.61 to -0.66 m from Hour 3.4 to 8) to reach the steady state (also evident in the experimental results). This phenomenon was termed "overshoot" previously, i.e., the freshwater-seawater interface temporarily extends further than the final steady-state position. Previous modeling studies (Chang et al., 2011; Watson et al., 2010) and experiments (Morgan et al., 2013), which were all for isothermal conditions, suggested that instantaneous sea level rise could incur an overshoot phenomenon. The present overshoot phenomenon results from asynchronous adjustment of the salinity and temperature distributions. The hydraulic diffusivity is larger than salt and heat diffusivity by several orders of magnitude (Ghuman & Lal, 1985; Shih, 2017). Freshwater injection produced a pressure wave that propagated through the aquifer. This induced a rapid response in the lateral hydraulic gradient (Figure S3). As a result, saltwater wedge started to move seaward. The lagged heat transport gradually heated up the aquifer (both water and porous medium). The reduction in fluid viscosity due to higher temperatures increased the hydraulic conductivity along with the flow path of the injected freshwater (Figure S4). Based

on Darcy's law ($Q = -KA\,\mathrm{d}h/\mathrm{d}x$ where Q is the flux, A is the cross-sectional flow area, K is the hydraulic conductivity and $\mathrm{d}h/\mathrm{d}x$ is the lateral hydraulic gradient), the decreased hydraulic gradient increased the seawater intrusion since the total freshwater discharge (inland freshwater input and recharge flux) was fixed (Figures S3 and S4). Overall, this overshoot was remarkable and long-lasting. The toe location and area of saltwater wedge exceeded those at the final steady state by 0.05 m and 0.013 m^2, respectively, amounting to 19.2% and 27.7% of the change between beginning and final steady states. The retreat took around 3.4 h and the reverse process after the overshoot peak took more than 2.8 h (i.e., response time minus retreating period).

We further numerically explored the response of salinity distributions to freshwater recharge in large-scale confined aquifers (400-m long and 100-m high). Both homogenous (with an intrinsic permeability of 10^{-11} m^2) and heterogeneous (the distribution of intrinsic permeability was lognormal and with a mean value of 10^{-11} m^2, based on the approach of Bellin and Rubin (1996)) confined aquifers were considered. The results were consistent with those at the laboratory-scale (see supplementary materials). In both the homogenous and heterogeneous confined aquifers, the hotter freshwater recharge induced saltwater wedges further landward (further seawater intrusion). The areas of saltwater wedges for T_{in} = 40°C nearly doubled those for T_{in} = 10°C, consistent with the extent of thermal impact demonstrated by the experiment. Apparent overshoot processes also appeared in both the toe locations and saltwater wedge areas, which exceeded around 20% of the associated changes between the two steady states. Most significantly, the rebound periods after the overshoot peaks were long-lasting and took around 3 y.

4. Concluding remarks

Coastal areas face increasing threats from human activities and climate change. Increases in groundwater extraction as well as sea level rise due to global warming are ongoing issues. Seawater intrusion into coastal aquifers is ubiquitous and challenges socioeconomic development in densely populated coastal areas. Our numerical results at both laboratory and large scales demonstrated that 40°C hot water recharge led to a doubling of the area of saltwater wedge compared with that for 10°C cold water. This thermal impact is significant, suggesting that applications of artificial freshwater recharge should consider the temperature difference between recharge water and aquifers. Numerical models based on isothermal conditions are unable to predict the performance of artificial groundwater recharge schemes. In engineering practice, such schemes would perform better using cold water as low temperatures could lower the hydraulic conductivity of aquifers and thus enhance the performance of hydraulic barriers in mitigating seawater intrusion.

We demonstrated that hot freshwater recharge could induce an overshoot phenomenon with respect to the toe location and saltwater wedge area. This demonstrated the complexity and vulnerability of coastal aquifers. Due to the lengthy rebound period, in practice the extent of in situ seawater retreat caused by artificial freshwater recharge may be overestimated as the freshwater-seawater interface may intrude back with a changing thermal regime. Based on our results, the reverse process was long-lasting and similar to the period for seawater retreat. Field measurements could consider not only flow and salinity distributions but also long-term temperature distributions.

The present results are based on 2D confined aquifers in a rectangular configuration. Natural aquifers likely include discrete confining layers with irregular shapes. In practice, multiple

recharge wells are often installed, leading to a 3D system (Allow, 2011). We considered continuous freshwater recharge with constant temperature, although in the field both flux and temperature of recharge water are likely variable. Sea levels are dynamic with both tides and waves, which would enhance the solute and heat mixing in aquifers (Nguyen et al., 2020; Xin et al., 2010). Nevertheless, the present study has revealed the significant thermal impact on both flow and solute transport in coastal aquifers that should be considered in management of coastal groundwater resources and restoration of groundwater systems.

Acknowledgments

This work was supported by the National Natural Science Foundation of China (U2040204) and Natural Science Foundation of Jiangsu Province (BK20200020).

References

Abd-Elhamid, H. F., & Javadi, A. A. (2011). A cost-effective method to control seawater intrusion in coastal aquifers. *Water Resources Management, 25*(11), 2755-2780. https://doi.org/10.1007/s11269-011-9837-7

Allow, K. A. (2011). The use of injection wells and a subsurface barrier in the prevention of seawater intrusion: A modelling approach. *Arabian Journal of Geosciences, 5*(5), 1151-1161. https://doi.org/10.1007/s12517-011-0304-9

Armanuos, A. M., Al-Ansari, N., & Yaseen, Z. M. (2020). Assessing the effectiveness of using recharge wells for controlling the saltwater intrusion in unconfined coastal aquifers with sloping beds: Numerical study. *Sustainability, 12*(7), 2685. https://doi.org/10.3390/su12072685

Ballesteros, B. J., Morell, I., García-Menéndez, O., & Renau-Pruñonosa, A. (2016). A standardized index for assessing seawater intrusion in coastal aquifers: The SITE index. *Water Resources Management, 30*(13), 4513-4527. https://doi.org/10.1007/s11269-016-1433-4

Barlow, P. M., & Reichard, E. G. (2009). Saltwater intrusion in coastal regions of North America. *Hydrogeology Journal, 18*(1), 247-260. https://doi.org/10.1007/s10040-009-0514-3

Bellin, A., & Rubin, Y. (1996). HYDRO_GEN: A spatially distributed random field generator for correlated properties. *Stochastic Hydrology and Hydraulics, 10*(4), 253-278. https://doi.org/10.1007/BF01581869

Botero-Acosta, A., & Donado, L. D. (2015). Laboratory scale simulation of hydraulic barriers to seawater intrusion in confined coastal aquifers considering the effects of stratification. *Procedia Environmental Sciences, 25*, 36-43. https://doi.org/10.1016/j.proenv.2015.04.006

Bouri, S., & Dhia, H. B. (2010). A thirty-year artificial recharge experiment in a coastal aquifer in an arid zone: The Teboulba aquifer system (Tunisian Sahel). *Comptes Rendus Geoscience, 342*(1), 60-74. https://doi.org/10.1016/j.crte.2009.10.008

Chang, S. W., & Clement, T. P. (2012). Experimental and numerical investigation of saltwater intrusion dynamics in flux-controlled groundwater systems. *Water Resources Research, 48*(9). https://doi.org/10.1029/2012wr012134

Chang, S. W., & Clement, T. P. (2013). Laboratory and numerical investigation of transport processes occurring above and within a saltwater wedge. *Journal of Contaminant Hydrology, 147*, 14-24. https://doi.org/10.1016/j.jconhyd.2013.02.005

Chang, S. W., Clement, T. P., Simpson, M. J., & Lee, K.-K. (2011). Does sea-level rise have an impact on saltwater intrusion? *Advances in Water Resources, 34*(10), 1283-1291. https://doi.org/10.1016/j.advwatres.2011.06.006

Costall, A. R., Harris, B. D., Teo, B., Schaa, R., Wagner, F. M., & Pigois, J. P. (2020). Groundwater throughflow and seawater intrusion in high quality coastal aquifers. *Scientific Reports, 10*(1), 9866. https://doi.org/10.1038/s41598-020-66516-6

Engineering ToolBox. (2003a). Specific heat of some common substances. Retrieved from https://www.engineeringtoolbox.com/specific-heat-capacity-d_391.html. Last accessed 14 August 2020.

Engineering ToolBox. (2003b). Thermal conductivity of selected materials and gases. Retrieved from https://www.engineeringtoolbox.com/thermal-conductivity-d_429.html. Last accessed 14 August 2020.

Ferguson, G., & Gleeson, T. (2012). Vulnerability of coastal aquifers to groundwater use and climate change. *Nature Climate Change, 2*(5), 342-345. https://doi.org/10.1038/nclimate1413

Ghuman, B. S., & Lal, R. (1985). Thermal conductivity, thermal diffusivity, and thermal capacity of some Nigerian soils. *Soil Science, 139*(1), 74-80. https://doi.org/10.1097/00010694-198501000-00011

Goswami, R. R., & Clement, T. P. (2007). Laboratory-scale investigation of saltwater intrusion dynamics. *Water Resources Research, 43*(4), W04418. https://doi.org/10.1029/2006wr005151

Henry, H. R. (1964). Effects of dispersion on salt encroachment in coastal aquifers. *U.S. Geological Survey, Water-Supply Paper 1613-C*, 70–84. Retrieved from https://pubs.usgs.gov/wsp/1613c/report.pdf.

Hughes, J. D., & Sanford, W. E. (2004). SUTRA-MS: A version of SUTRA modified to simulate heat and multiple-solute transport. *U.S. Geological Survey Open-File Report 2004-1207*, 141 p. Retrieved from https://water.usgs.gov/nrp/gwsoftware/SutraMS/SutraMS.html. Last accessed 14 August 2020.

Hunt, A. G., Skinner, T. E., Ewing, R. P., & Ghanbarian-Alavijeh, B. (2011). Dispersion of solutes in porous media. *The European Physical Journal B, 80*(4), 411-432. https://doi.org/10.1140/epjb/e2011-10805-y

Hunt, B. (1985). Some analytical solutions for seawater intrusion control with recharge wells. *Journal of Hydrology, 80*(1-2), 9-18. https://doi.org/10.1016/0022-1694(85)90072-1

Hussain, M. S., Abd-Elhamid, H. F., Javadi, A. A., & Sherif, M. M. (2019). Management of seawater intrusion in coastal aquifers: A review. *Water, 11*(12), 2467. https://doi.org/10.3390/w11122467

Jamshidzadeh, Z., Tsai, F. T. C., Mirbagheri, S. A., & Ghasemzadeh, H. (2013). Fluid dispersion effects on density-driven thermohaline flow and transport in porous media. *Advances in Water Resources, 61*, 12-28. https://doi.org/10.1016/j.advwatres.2013.08.006

Kuan, W. K., Jin, G., Xin, P., Robinson, C., Gibbes, B., & Li, L. (2012). Tidal influence on seawater intrusion in unconfined coastal aquifers. *Water Resources Research, 48*(2), W02502. https://doi.org/10.1029/2011wr010678

Lu, C., Shi, W., Xin, P., Wu, J., & Werner, A. D. (2017). Replenishing an unconfined coastal aquifer to control seawater intrusion: Injection or infiltration? *Water Resources Research, 53*(6), 4775-4786. https://doi.org/10.1002/2016wr019625

Luyun, R., Jr., Momii, K., & Nakagawa, K. (2011). Effects of recharge wells and flow barriers on seawater intrusion. *Ground Water, 49*(2), 239-249. https://doi.org/10.1111/j.1745-6584.2010.00719.x

Mahesha, A. (1996a). Steady-state effect of freshwater injection on seawater intrusion. *Journal of Irrigation and Drainage Engineering, 122*(3), 149-154. https://doi.org/10.1061/(ASCE)0733-9437(1996)122:3(149)

Mahesha, A. (1996b). Transient effect of battery of injection wells on seawater intrusion. *Journal of Hydraulic Engineering, 122*(5), 266-271. https://doi.org/10.1061/(ASCE)0733-9429(1996)122:5(266)

Mao, X., Enot, P., Barry, D. A., Li, L., Binley, A., & Jeng, D.-S. (2006). Tidal influence on behaviour of a coastal aquifer adjacent to a low-relief estuary. *Journal of Hydrology, 327*(1-2), 110-127. https://doi.org/10.1016/j.jhydrol.2005.11.030

Morgan, L. K., Stoeckl, L., Werner, A. D., & Post, V. E. A. (2013). An assessment of seawater intrusion overshoot using physical and numerical modeling. *Water Resources Research, 49*(10), 6522-6526. https://doi.org/10.1002/wrcr.20526

Nguyen, T. T. M., Yu, X., Pu, L., Xin, P., Zhang, C., Barry, D. A., & Li, L. (2020). Effects of temperature on tidally influenced coastal unconfined aquifers. *Water Resources Research, 56*(4). https://doi.org/10.1029/2019wr026660

Pu, L., Xin, P., Nguyen, T. T. M., Yu, X., Li, L., & Barry, D. A. (2020). Thermal effects on flow and salinity distributions in coastal confined aquifers. *Water Resources Research, 56*(10). https://doi.org/10.1029/2020wr027582

Robinson, C. E., Xin, P., Santos, I. R., Charette, M. A., Li, L., & Barry, D. A. (2018). Groundwater dynamics in subterranean estuaries of coastal unconfined aquifers: Controls on submarine groundwater discharge and chemical inputs to the ocean. *Advances in Water Resources, 115*, 315-331. https://doi.org/10.1016/j.advwatres.2017.10.041

Shi, L., & Jiao, J. J. (2014). Seawater intrusion and coastal aquifer management in China: A review. *Environmental Earth Sciences, 72*(8), 2811-2819. https://doi.org/10.1007/s12665-014-3186-9

Shih, D. C.-F. (2017). Hydraulic diffusivity in a coastal aquifer: Spectral analysis of groundwater level in responses to marine system. *Stochastic Environmental Research and Risk Assessment, 32*(2), 311-320. https://doi.org/10.1007/s00477-017-1420-1

Singh, A. (2014). Optimization modelling for seawater intrusion management. *Journal of Hydrology, 508*, 43-52. https://doi.org/10.1016/j.jhydrol.2013.10.042

Van Lopik, J. H., Hartog, N., Zaadnoordijk, W. J., Cirkel, D. G., & Raoof, A. (2015). Salinization in a stratified aquifer induced by heat transfer from well casings. *Advances in Water Resources, 86*, 32-45. https://doi.org/10.1016/j.advwatres.2015.09.025

Watson, T. A., Werner, A. D., & Simmons, C. T. (2010). Transience of seawater intrusion in response to sea level rise. *Water Resources Research, 46*(12), W12533. https://doi.org/10.1029/2010wr009564

Werner, A. D. (2009). A review of seawater intrusion and its management in Australia. *Hydrogeology Journal, 18*(1), 281-285. https://doi.org/10.1007/s10040-009-0465-8

Werner, A. D., Bakker, M., Post, V. E. A., Vandenbohede, A., Lu, C., Ataie-Ashtiani, B., et al. (2013). Seawater intrusion processes, investigation and management: Recent advances and future challenges. *Advances in Water Resources, 51*, 3-26. https://doi.org/10.1016/j.advwatres.2012.03.004

Xin, P., Robinson, C., Li, L., Barry, D. A., & Bakhtyar, R. (2010). Effects of wave forcing on a subterranean estuary. *Water Resources Research, 46*(12), W12505. https://doi.org/10.1029/2010wr009632

Table 1. Parameter values used for the laboratory-scale confined aquifer.

Symbol	Parameter	Value	Unit
ϕ	porosity	0.39*	-
k	intrinsic permeability	4.5×10^{-10}#	m^2
α_L	longitudinal dispersivity	0.01	m
α_T	transverse dispersivity	0.001	m
c_f	fluid specific heat	4182	J/kg/℃
c_s	solid matrix specific heat	840	J/kg/℃
λ_f	fluid thermal conductivity	0.6	J/m/℃/s
λ_s	solid thermal conductivity	2.3*	J/m/℃/s
D_M	molecular diffusivity	10^{-9}	m^2/s
α	compressibility of solid matrix	10^{-7}	Pa^{-1}
β	compressibility of fluid	4.47×10^{-10}	Pa^{-1}

*Measured value. #Adjusted value (to match the experimental result before freshwater recharge). The measured intrinsic permeability was 5×10^{-10} m^2. The longitudinal and transverse dispersivities were selected from Hunt et al. (2011). The thermal parameters were selected from the Engineering ToolBox (2003a, 2003b).

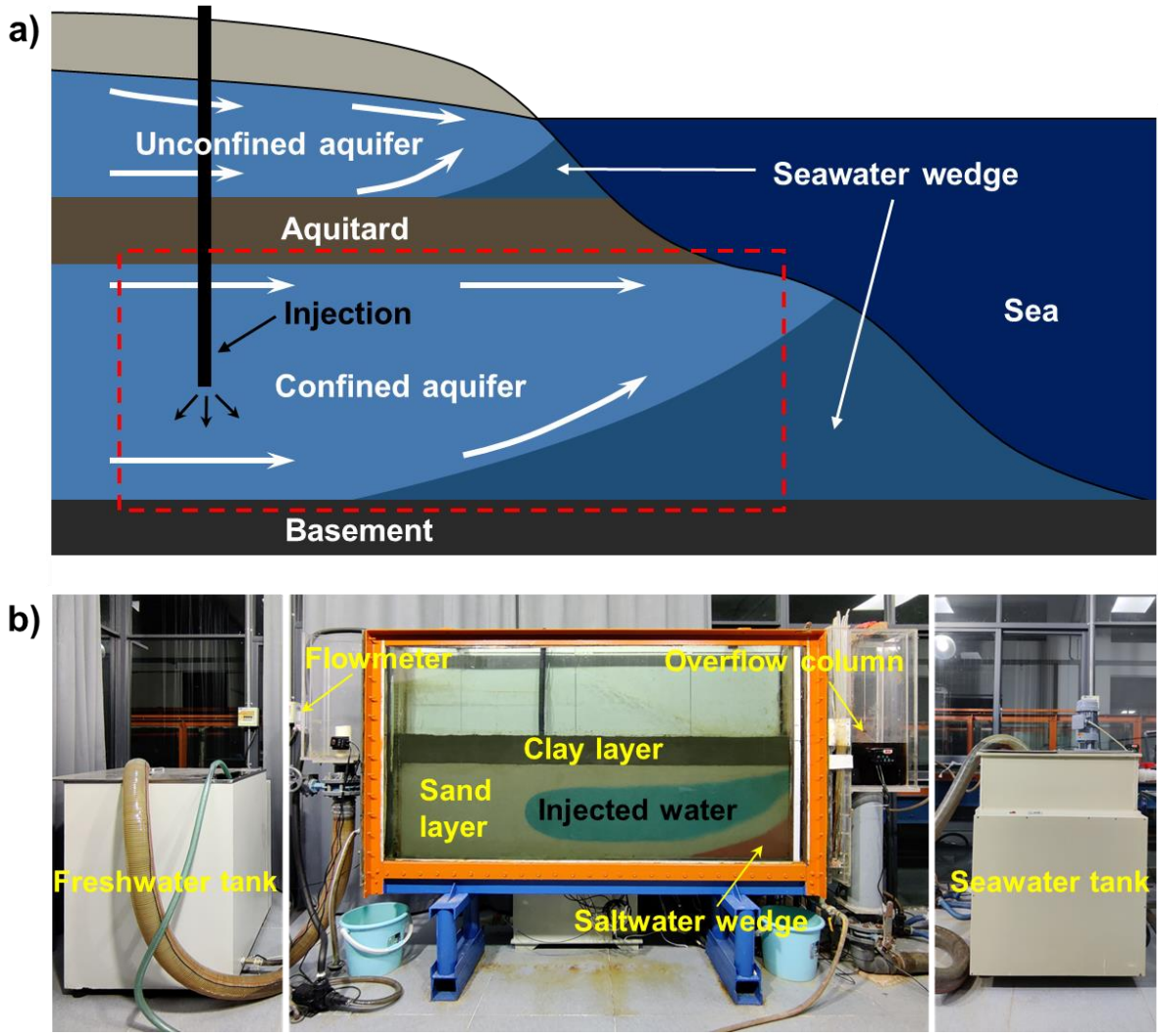

Figure 1. (a) Conceptual diagram of coastal cross-shore confined-unconfined aquifers and major flow processes; (b) Laboratory experimental apparatus for a confined aquifer (illustrated by a red square in (a)). The experimental aquifer was set up in a heat-insulated apparatus. Left and right of the aquifer are two temperature-controlled tanks for freshwater and seawater, respectively.

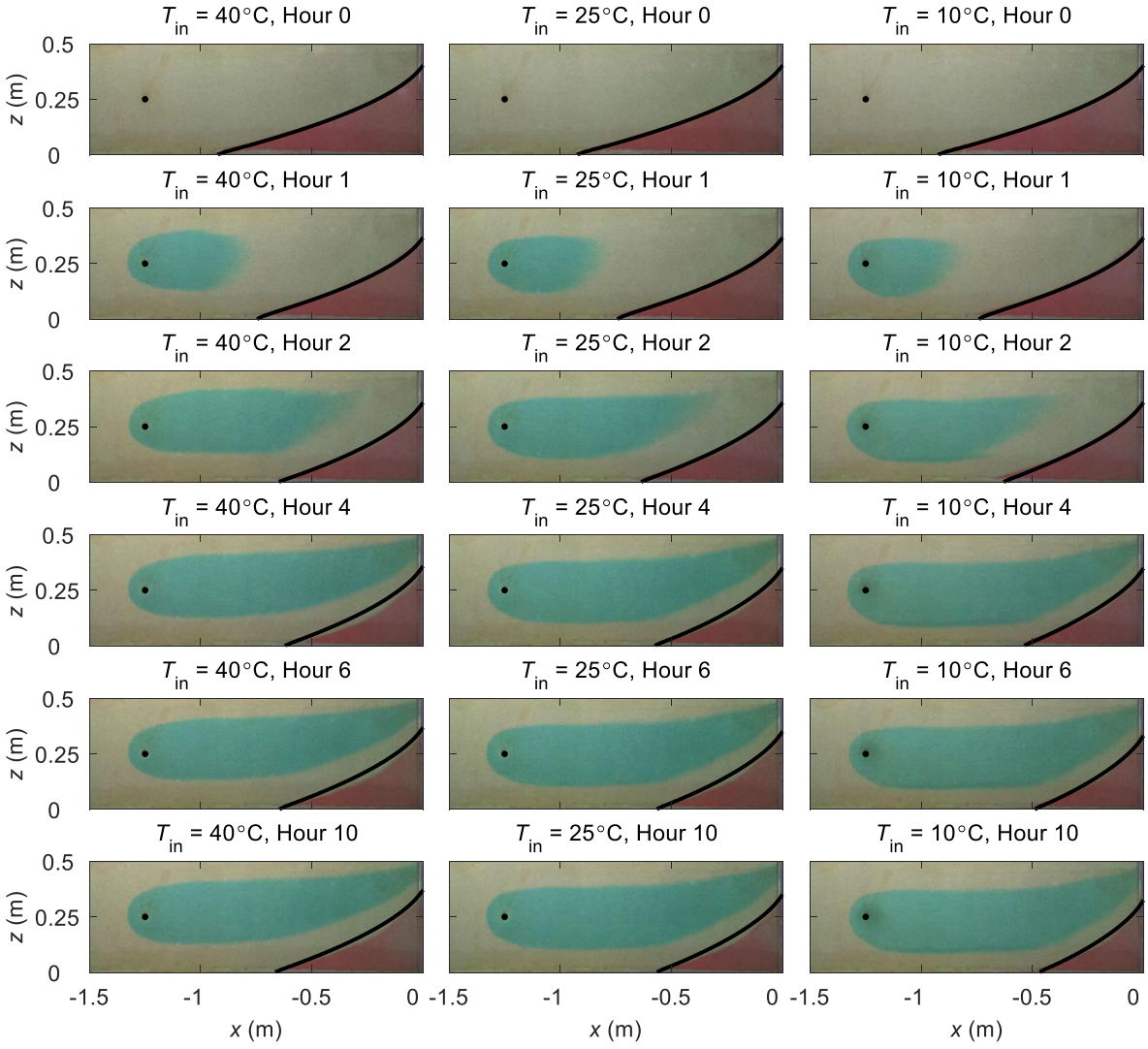

Figure 2. Snapshots of the experimental salinity distributions after the freshwater injection. Red indicates seawater and blue indicates injected freshwater. The black lines show the simulated interface between freshwater and seawater (50% seawater salinity isoline). The black dots show the injection points. Left-side, middle and right-side panels are, respectively, for the temperature of the injected water (T_{in}) set at 40℃, 25℃ and 10℃.

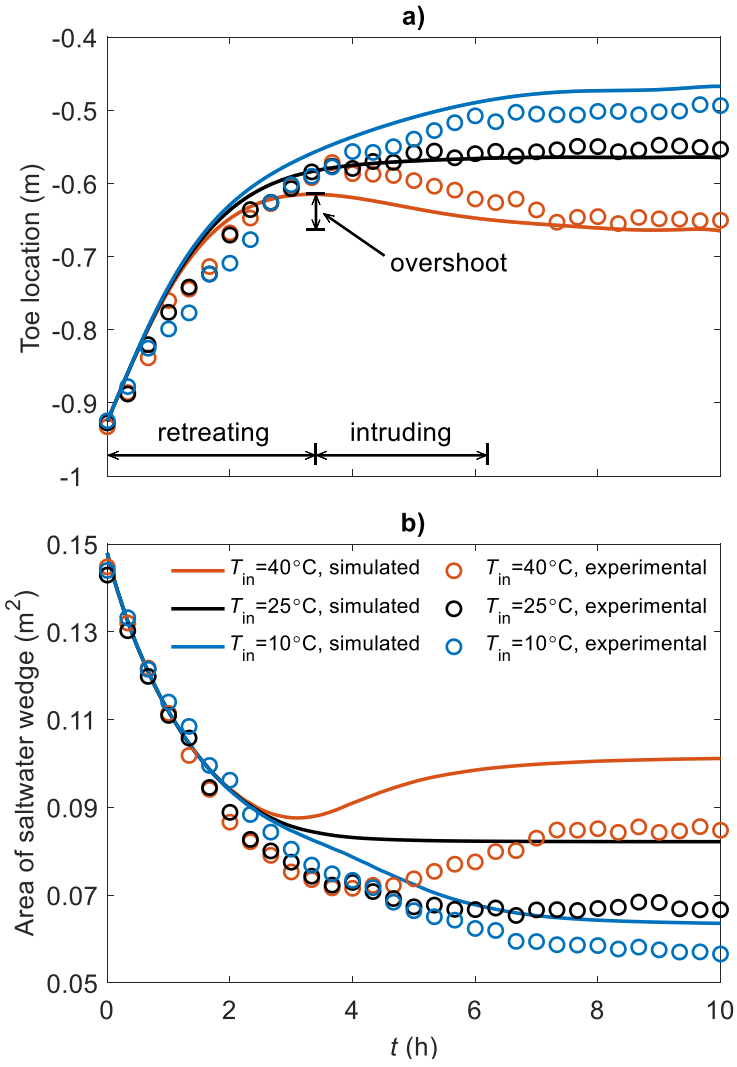

Figure 3. Variations of toe locations (a) and areas of saltwater wedge (b) in the aquifers after the freshwater injection. Both the experimental and simulated results are given. T_{in} indicates the temperature of the injected freshwater.